

# Electrical Conductivity of Supercooled Aqueous Mixtures of Trehalose with Sodium Chloride

Danforth P. Miller,<sup>†</sup> Paul B. Conrad,<sup>†</sup> Silvana Fucito,<sup>‡</sup> Horacio R. Corti,<sup>‡,§,||</sup> and Juan J. de Pablo<sup>\*,†</sup>

Department of Chemical Engineering, University of Wisconsin—Madison, 1415 Engineering Drive, Madison, Wisconsin 53706, Unidad de Actividad Química, Comisión Nacional de Energía Atómica, Av. General Paz 1499, (1650) San Martín, Buenos Aires, Argentina, and Escuela de Ciencia y Tecnología, Universidad Nacional de General San Martín, Buenos Aires, Argentina

Received: February 24, 2000; In Final Form: August 10, 2000

The viscosity and electrical conductivity of aqueous solutions of trehalose and other saccharides containing 1:1 electrolytes have been measured. The decrease in the molar conductivity of each of these electrolytes with increasing viscosity is less than that predicted by Walden's rule. Instead, the empirical relation  $\Lambda\eta^\alpha = \text{constant}$ , which has already been found for other glass-forming liquids, holds for these mixtures. The microscopic origin of the deviation from the viscous friction model could be related to the presence of local heterogeneities in the distribution of water about the ions. This hypothesis is supported by the results of extensive molecular simulations. The temperature dependence of the Walden product of NaCl in aqueous trehalose mixtures indicates that this salt is fully dissociated close to the glass-transition temperature ( $T_g$ ).

## Introduction

The ability of trehalose ( $\alpha$ -D-glucopyranosyl- $\alpha$ -D-glucopyranoside) to preserve the structure and function of biomolecules in aqueous glassy matrices is well-known.<sup>1,2</sup> The protective mechanism is a combination of the high glass-transition temperature ( $T_g$ ) of trehalose and its concentrated aqueous trehalose solutions<sup>3</sup> and the ability of trehalose to replace water in the vicinity of biological structures.<sup>4,5</sup>

Most biological systems of interest contain ionic solutes. Unfortunately, available studies of trehalose solutions have not examined the effect of such solutes in a systematic manner. This lack of information has motivated us to study ionic mobility and how ionic solutes modify the thermophysical properties of trehalose solutions. Recently,<sup>6</sup> we studied the effect of NaCl and Na<sub>2</sub>B<sub>4</sub>O<sub>7</sub> (Borax) on the  $T_g$  and viscosity of aqueous trehalose. We concluded that the formation of chemical complexes between trehalose and borate contributes to the dramatic increase of  $T_g$  and viscosity of the mixtures. Noncomplexing salts, such as NaCl, were found to have only a minor effect on these properties.

In a recent work,<sup>7</sup> a simple random-energy model was used to predict the effect of ionic impurities on  $T_g$ . Experimental data<sup>6,8,9</sup> indicate that the model considerably overestimates the effect of charged solutes on  $T_g$ . Theory and experiment could be reconciled by considering the extent of ion association in the supercooled and glassy regimes. We have therefore measured the electrical conductivity of supercooled aqueous solutions of trehalose containing NaCl. Our aim was to detect a possible increase in the degree of ionic association as temperature decreases toward  $T_g$ .

Glass-forming liquids have traditionally been classified as fragile or strong liquids.<sup>10</sup> Fragile liquids exhibit pronounced changes in their transport properties (e.g., viscosity, diffusivity) as  $T_g$  is approached. Trehalose solutions have been shown to be fragile,<sup>11</sup> and we are interested in the mechanism of conduction of simple ions in such systems because it is likely to be of fundamental importance for applications relevant to biological stabilization.

Perhaps the simplest model to describe the temperature dependence of transport properties of a solute is the continuum friction model. In this model, the diffusion coefficient ( $D$ ) of a spherical solute of hydrodynamic radius  $r$  in a solvent of viscosity,  $\eta$ , is given by the Stokes–Einstein relation:<sup>12</sup>

$$D = \frac{k_B T}{A r \eta} \quad (1)$$

Its electrical conductivity counterpart is the Walden equation for the molar conductivity ( $\Lambda$ )

$$\Lambda = \frac{z^2 e F}{A r \eta} \quad (2)$$

where, for an ionic solute,  $r$  is calculated from the relation  $1/r = 1/r^+ + 1/r^-$ , the sum of the reciprocal radii of the ions,  $k_B$  is Boltzmann's constant,  $F$  is Faraday's constant,  $e$  is the charge of an electron, and  $z$  is the valence. In eqs 1 and 2,  $A$  is a constant whose value depends on the boundary conditions employed for friction;  $A$  is  $6\pi$  for stick and  $4\pi$  for slip boundary conditions at the solvent/solute interface.

These relations are known to be valid in liquids when the size of the solute is large compared to that of the solvent molecules. For small ionic solutes, however, the dielectric friction mechanism becomes important, thereby resulting in a reduction of the transport coefficients.

In fragile supercooled liquids such as aqueous trehalose, the viscosity changes rapidly with temperature. This allows the study

\* Corresponding author. E-mail: depablo@enr.wisc.edu. Fax: (608) 262-5434.

<sup>†</sup> University of Wisconsin—Madison.

<sup>‡</sup> Comisión Nacional de Energía Atómica.

<sup>§</sup> Universidad Nacional de General San Martín.

<sup>||</sup> E-mail: hrcorti@cnea.gov.ar.

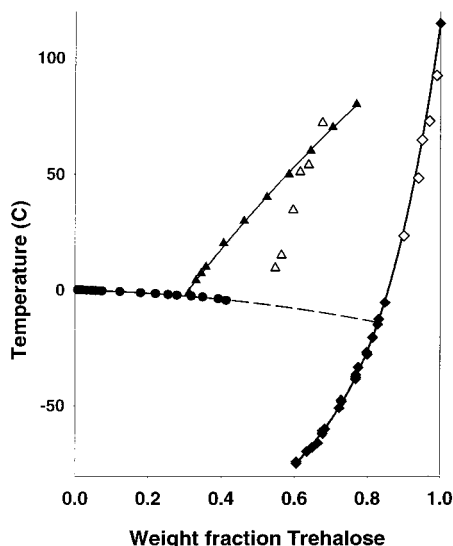


**Figure 1.** Phase diagram of aqueous trehalose showing the supercooled liquid region studied in this work: (●) freezing point depression, (▲) solubility, (△) solubility (Nicolajsen and Hvidt, 1994),<sup>44</sup> (◆) glass-transition temperature, and (◇) glass-transition temperature (Saleki-Gerhardt, 1993).<sup>45</sup> All data from ref 11, except where noted.

of a modest temperature range in which dynamic properties change by several orders of magnitude. Because of the thermodynamic metastability of these solutions, it is possible to perform electrical conductivity measurements using standard methods employed for aqueous electrolytes. Figure 1 represents the phase diagram of aqueous trehalose. This figure also shows the glass-transition temperature of solutions between 55 and 75 wt % trehalose, corresponding to the composition range studied in this work. The glass-transition temperature of the trehalose/water/ion mixtures studied is quite close to that of the trehalose/water composition, as has been discussed in a previous work.<sup>6</sup> As the temperature approaches  $T_g$ , the viscosity becomes very large and one would expect the viscous friction mechanism to be replaced by an activated hopping mechanism that is characteristic of the solid state.

## Experimental Section

**Materials and Methods.** D-(+)-Trehalose dihydrate, maltose monohydrate, glucose, and sucrose were obtained from Pfanzstiel Laboratories (Waukegan, IL), 99.6%, 99.9%, 99.9%, and 99.8%, respectively. Sodium, lithium, potassium, calcium, and magnesium (hexahydrate) chlorides (Aldrich Chemical Co., 99%, 99.99%, 99.999%, 99.99%, 99.99%) were used for all experimental work. Ethanol (100%) and potassium iodide (99.99%) were obtained from Aaper Alcohol and Chemical Co. (Shelbyville, KY) and Aldrich, respectively. All water was prepared by a Milli-Q filtration system. All solutions were prepared gravimetrically on an analytical microbalance; the result of each weighing was adjusted to vacuo by the appropriate buoyancy factor. Most solutions required heating and mixing to dissolve the solute. To enable dissolution of solutes, most compositions were heated in sealed glass vials.

The absolute water content of trehalose dihydrate was measured using Karl Fischer coulometric titration (Metrohm, model 737). The water content of all solutes was accounted for in the preparation of aqueous compositions.

**Viscometry.** Viscosities of solutions were measured using a Bohlin CVO controlled-stress rheometer with a coaxial cylinder ("cup and bob") measurement geometry, as described in a previous work.<sup>11</sup> A 14 mm diameter bob was used for highly

viscous samples, while a 25 mm bob was used for the less viscous solutions ( $\eta < 0.5$  Pa·s). The minimum temperature allowed by the cooling system was  $-20$  °C. The shear stress was adjusted between 0.15 and 7000 Pa to provide a shear rate between 1 and  $40$  s<sup>-1</sup>. For measurements at temperatures above 10 °C, a drop of low viscosity silicone oil (5 mPa·s) was placed on the liquid surface to reduce evaporation of water.

Owing to the low concentration of NaCl in the solutions used in all experiments, their viscosities could be approximated by that of the corresponding binary aqueous saccharide solutions at the same concentration.<sup>6</sup> However, to avoid uncertainties resulting from interpolation, we have measured the viscosities at the same compositions and temperatures used in the conductivity measurements.

The glass-transition temperature was measured using differential scanning calorimetry. Details of these measurements are provided in a previous work.<sup>6</sup>

**Conductivity.** Glass conductivity cells with platinized platinum electrodes were used for all measurements. The cells were immersed in a thermostated bath whose temperature was controlled better than 0.1 K over the course of the experiment. The cell constants were determined using aqueous KCl at 25 °C and KI/ethanol solutions at subambient temperatures, whose molar conductivity is accurately known as a function of temperature.<sup>13</sup> The values of the cell constants ranged from 0.1 to 1.0 cm<sup>-1</sup> at 25 °C and changed less than 5% over the temperature range used in this work ( $-20$  to 25 °C). In all cases, the specific conductivity of the binary trehalose/water mixture was subtracted from the specific conductivity of the aqueous trehalose/NaCl solutions to eliminate the contribution of ionic impurities present in the trehalose or dissolved carbon dioxide in the water used to prepare the solutions.

**Molecular Simulations.** The molecular simulations in this work were carried out using an isothermal molecular dynamics algorithm. We used a fully flexible SPC-type water model<sup>14</sup> with harmonic bond potentials.<sup>15</sup> The trehalose model was based on the OPLS force field.<sup>16</sup>

All the models used in this work include Lennard-Jones 6-12, Coulombic, and bonded interactions. The Lennard-Jones parameters were chosen from the above references; the cutoff distance in this work was at least  $2\sigma$  (7 Å) for all atoms. The usual Lorentz-Bertholet combining rules were used to calculate cross-interaction parameters. A long-range correction was applied to the energy and virial to account for the truncation of the potential at the cutoff. The direct Coulombic interactions (i.e., those within the Lennard-Jones cutoff radius) were calculated using an Ewald-sum method with a convergence parameter of  $0.36$  Å<sup>-1</sup>. Reciprocal space Coulombic contributions were included by means of a "smooth particle mesh Ewald" (PME) method.<sup>17,18</sup> The PME method was used with eighth-order splines and 16 mesh lines (spacing of 1.0–1.3 Å) in each dimension. A reversible multiple time scales method (r-RESPA)<sup>19</sup> was used to accelerate the performance of molecular dynamics simulations. In our implementation, a double-RESPA method was used to prevent deviation of the system pressure. The potential energy was separated into three parts: bonded interactions (bonds, bending, and torsion), short-range interactions (i.e., nonbonded interactions within the cutoff radius), and long-range interactions (i.e., reciprocal Coulombic calculations). One step consisted of four updates of the bonded interactions, two updates of the short-range interactions, and one update of the long-range interactions. The total time step used was 1 fs (i.e., the bonded and short-range interactions were updated every 0.25 and 0.5 fs, respectively). Included in this

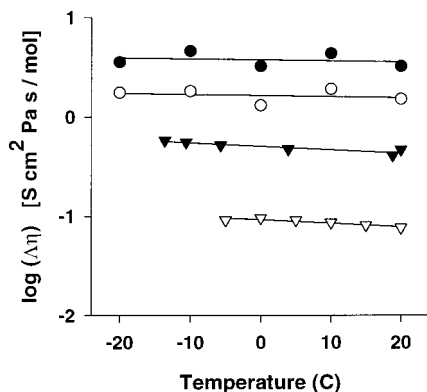


**Figure 2.** Walden product of NaCl in aqueous trehalose as a function of temperature at different trehalose concentrations: (●) 74.8, (○) 71.0, (▼) 57.9, and (▽) 34.5 wt %. In all cases, the NaCl concentration is 0.01 M.

method was a chain of five Nosé–Hoover thermostats using the method described by Martyna et al.<sup>20</sup> Following Nosé,<sup>21</sup> the frequency of the thermostat fluctuations was chosen to be 0.002 fs<sup>-1</sup>. All simulations were carried out at 300 K. The box length for the NVTMD simulations was chosen from experimentally measured densities. The system sizes depended on the composition of the solution under investigation. For the most dilute (with respect to trehalose) case, 6 wt % trehalose, 300 water molecules were used with a single trehalose molecule, 19 Na ions, and 19 Cl ions. For the 60 wt % trehalose case, the mixture contained 63 water molecules, 5 trehalose molecules, 4 Na ions, and 4 Cl ions. Intermediate compositions were between these two extremes. The NaCl concentration was maintained at 0.06 *m* in all cases. The lengths of the NVTMD simulations were at least  $2 \times 10^6$  steps (2 ns). More concentrated solutions required simulations as long as  $5 \times 10^7$  steps (50 ns) in order to reach the diffusive regime.

## Results and Discussion

**Conductivity of NaCl in Trehalose Aqueous Solutions as a Function of Temperature.** The conductivity and viscosity of aqueous NaCl/trehalose solutions were measured at different temperatures. The range of temperature for each solution was chosen to avoid ice crystallization. The higher the concentration of trehalose, the lower the temperature that could be achieved without ice crystallization. Thus, at the highest concentrations, the measurements extended down to  $-20$  °C.

The Walden product of several different trehalose/water/NaCl solutions as a function of temperature is shown in Figure 2. The linear regressions show that, for these solutions, the Walden product is relatively insensitive to temperature; it increases only slightly as temperature decreases. This behavior confirms that the dissociation of NaCl at low temperatures (supercooled solutions) is complete, as it is in water at room temperature.

**Conductivity of NaCl in Trehalose and Other Saccharides in Aqueous Solutions at 25 °C.** The molar conductivities ( $\Lambda$ ) and viscosities ( $\eta$ ) at 25 °C of aqueous NaCl solutions containing between 20 and 75 wt % trehalose are reported in Table 1. The concentration of NaCl used in these measurements was always close to 0.01 M, which ensures that the molar conductivities are close to the values at infinite dilution. The molar conductivity of NaCl at infinite dilution in water<sup>22</sup> is included in Table 1 for comparison.

As expected, the molar conductivity decreases with the trehalose concentration owing to the increase of the viscosity.

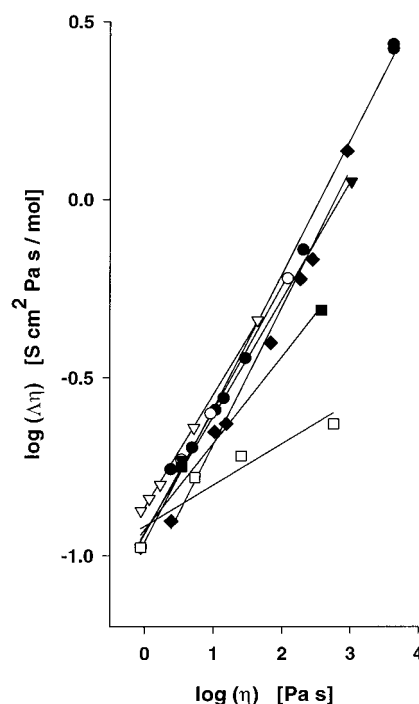


**Figure 3.** Walden plot for the conductivity of aqueous solutions of (●) trehalose/NaCl, (○) maltose/NaCl, (▼) sucrose/NaCl, (▽) sucrose/KCl (ref 23), (■) glucose/NaCl, (□) glycerol/NaCl, and (◆) trehalose/LiCl. In all cases, the NaCl or LiCl concentration was nominally 0.01 M.

**TABLE 1: Conductivity and Viscosity of Aqueous Trehalose/NaCl at 25 °C**

wt % trehalose	$C_{\text{NaCl}}$ (mM)	$\Lambda$ ( $\text{S}\cdot\text{cm}^2/\text{mol}$ )	$\eta$ (mPa·s)	Walden product ( $\text{S}\cdot\text{cm}^2\cdot\text{Pa}\cdot\text{s}/\text{mol}$ )
0.00	0.000	126.39	0.8904	0.1126
19.98	9.940	73.34	2.395	0.1756
34.98	9.932	41.52	4.87	0.202
45.00	9.955	24.24	10.67	0.259
53.95	9.942	12.53	28.9	0.362
58.98	9.967	7.87	64.3	0.506
64.96	9.957	3.86	202.1	0.779
70.96	9.952	1.41	860	1.21
74.97	9.977	0.613	4250	2.61

This is a consequence of the increase of the viscous friction, which can be described by Walden's "rule",  $\Lambda\eta = \text{constant}$ . According to eq 2, the Walden product,  $\Lambda\eta$ , in solutions containing different concentrations of trehalose should be constant, provided that only one mode of viscous friction is present and that the hydrodynamic size of each ion remains the same in all the solutions. However, as is shown in Figure 3, (at 25 °C) the Walden product of NaCl increases with the concentration of trehalose and viscosity.

To obey eq 1, the sizes of the Na<sup>+</sup> and Cl<sup>-</sup> ions in the aqueous-trehalose solutions should decrease from 0.75 nm in pure water to 0.34 nm in the 74.9 wt % trehalose solution. The latter value would imply that ions are either poorly hydrated or not hydrated, which is contrary to the results of molecular simulations. This suggests that Stokes' law is not valid in this highly viscous system. Therefore, we discuss the departures from Walden's rule in the context of dynamic heterogeneities, which are well-known to arise in pure systems as  $T_g$  is approached. An important point to note is that in several of the works described below the heterogeneities described occur in pure systems, whereas the current work describes chemical heterogeneities in an aqueous solution comprised of four different species.

**TABLE 2: Conductivity and Viscosity of Aqueous NaCl Containing Different Saccharides and Glycerol at 25 °C**

wt % saccharide	$C_{\text{NaCl}}$ (mM)	$\Lambda$ ( $\text{S}\cdot\text{cm}^2/\text{mol}$ )	$\eta$ ( $\text{mPa}\cdot\text{s}$ )	Walden product ( $\text{S}\cdot\text{cm}^2\cdot\text{Pa}\cdot\text{s}/\text{mol}$ )
sucrose 30.00	10.002	54.27	3.446	0.187
sucrose 73.98	9.496	1.20	1032	1.24
glucose 31.25	11.310	45.97	3.448	0.158
glucose 74.00	12.254	1.13	374	0.422
maltose 30.07	9.956	54.37	3.43	0.186
maltose 45.11	9.842	27.42	9.07	0.249
maltose 65.10	10.050	5.05	121.4	0.613
glycerol 48.89	9.980	30.98	5.405	0.167
glycerol 73.83	10.020	7.58	25.35	0.192
glycerol 97.86	10.000	0.440	566	0.249

**TABLE 3: Conductivity and Viscosity of Aqueous Trehalose/LiCl at 25 °C**

wt % trehalose	$C_{\text{LiCl}}$ (mM)	$\Lambda$ ( $\text{S}\cdot\text{cm}^2/\text{mol}$ )	$\eta$ ( $\text{mPa}\cdot\text{s}$ )	Walden product ( $\text{S}\cdot\text{cm}^2\cdot\text{Pa}\cdot\text{s}/\text{mol}$ )
0.00	0.000	107.27	0.8904	0.0955
27.09	10	51.288	2.44	0.1251
45.00	9.947	21.394	10.42	0.2229
49.99	10	15.202	15.45	0.2349
59.98	10	5.832	68.00	0.3966
64.95	9.966	3.255	184.1	0.615
66.74	10	2.451	277.4	0.6800
70.87	10	1.534	891.7	1.368

In early work, Stokes himself found nonconstant behavior in studies of the Walden product for KCl in aqueous sucrose.<sup>23</sup> He proposed the modified relation

$$\Lambda\eta^\alpha = \text{constant} \quad (3)$$

with  $\alpha = 0.7$  to describe his data; we have confirmed that this relation also holds for our trehalose/NaCl/water mixtures. Somewhat later, Moynihan<sup>24</sup> reported conductivity and viscosity results for melts of calcium nitrate and sodium thiosulfate salts, which give rise to the same fractional Walden behavior. Treiner and Fuoss<sup>25</sup> found that the power relation is equally applicable to quaternary salts in cyanoethylsucrose–acetonitrile mixtures and suggested that the local viscosity in the regions where the ions are able to move is much lower than the bulk viscosity.

Figure 3 includes the results of Stokes for KCl in sucrose/water solutions. These data, which extend between 1.18 and 43.8  $\text{mPa}\cdot\text{s}$  in viscosity, deviate from the Walden product ( $\alpha = 0.68$ ) almost identically to our results for NaCl in trehalose/water solutions ( $\alpha = 0.64$ ). Note that our results in trehalose/water cover a much wider range of viscosity (4.87–4250  $\text{mPa}\cdot\text{s}$ ).

The conductivity and viscosity of different aqueous saccharide/NaCl solutions was measured to study the effect of the molecular structure of the sugar on the Walden product and to test the validity of eq 3. We used nonreducing disaccharides (sucrose and trehalose), a reducing disaccharide (maltose), and a monosaccharide (glucose). The results summarized in Table 2 show that the behavior of the Walden product for NaCl is similar in all the sugars studied,  $\alpha = 0.64 \pm 0.02$ , as shown in Figure 3. For glucose, a monosaccharide, the deviation from the Walden rule is smaller ( $\alpha = 0.78$ ), while for glycerol the Walden product is nearly constant over the entire range of viscosity ( $\alpha = 0.91$ ). To compare the mobilities of different ions, we also measured the conductivity of LiCl in trehalose/water solutions. The results are summarized in Table 3, and the Walden product is shown in Figure 3. The molar conductivity of the trehalose/LiCl solutions is lower than that of the corresponding NaCl solutions, but the exponent of the empirical

relation (eq 3) is quite similar ( $\alpha = 0.66$ ) to that found for NaCl in aqueous disaccharides.

A discussion of the observed deviations from the Walden rule in terms of the effect of the dielectric friction,<sup>26</sup> which is expected to be important for these small ions, is not possible because we do not know how the Debye relaxation time changes with the solvent's composition. Note that Bagchi and Biswas recently demonstrated<sup>27</sup> with a molecular model that ultrafast solvation dynamics could be important in determining the mobility of ions in liquids.

It is interesting to compare these results with those reported for other glass-forming liquids in the supercooled regime. A fractional power Walden rule with  $\alpha = 0.63$  was found for the diffusion of Xe in water/sucrose solutions by Pollack<sup>28</sup> and more recently by Voronel et al.<sup>29</sup> for the electrical conductivity of ionic melts, with  $\alpha = 0.8 \pm 0.1$ . The behavior of ionic conductivity and diffusivity in salt-in-polymer electrolytes is more difficult to compare with the results of this work because ionic association is more pronounced in such systems.<sup>30,31</sup>

The translational diffusion of dye molecules in supercooled liquids and polymers has been studied by Ehlich and Sillescu<sup>32</sup> using Rayleigh scattering. They found that the temperature dependence of the diffusion coefficient and viscosity could be described by a Vogel–Tamman–Fulcher (VTF) equation with the same parameters  $B$  and  $T_0$

$$D = D_0 \exp\left(-\frac{\alpha B}{T - T_0}\right) \quad (4)$$

$$\eta = \eta_0 \exp\left(\frac{B}{T - T_0}\right) \quad (5)$$

In eq 4,  $\alpha$  is a parameter related to the decoupling of the diffusion of the probe molecule and the solvent matrix. Equations 4 and 5 imply that  $D\eta^\alpha = \text{constant}$ , which is the diffusional equivalent of eq 3.

Cicerone and Ediger<sup>33,34</sup> used a photobleaching technique to measure translational diffusion coefficients of probe molecules in *o*-terphenyl (OTP). They observed that, for probes that are the same size as OTP molecules, the product of translational diffusion and rotational correlation time increased by 2 orders of magnitude as  $T_g$  was approached. They explained their findings by suggesting that deeply supercooled OTP is spatially heterogeneous.

Rössler suggested<sup>35</sup> that a change of diffusion mechanism takes place at a crossover temperature,  $T_c$ , in the supercooled liquid ( $T_c \sim 1.8T_g$ ). At  $T > T_c$  the Stokes–Einstein equation is valid ( $\alpha = 1$ ), while, for  $T < T_c$ , there is a decoupling ( $\alpha < 1$ ) related to a dynamical phase transition observed at  $T = T_c$ . All viscosities and conductivities in this work were measured at temperatures above  $T_c$ .

Using a self-consistent mode-coupling theory, Bhattacharyya and Bagchi<sup>36</sup> studied the partial decoupling between translational diffusion of a solute molecule and the viscosity of the medium in the supercooled liquid regime.<sup>37,38</sup> Their theory accounts for coupled solute–solvent dynamics. At low degrees of supercooling, their theory predicts that the Stokes–Einstein relation is valid. However, at higher degrees of supercooling, the viscosity increases more rapidly than the decrease in the diffusion coefficient owing to a long-time tail in the dynamic structure factor. The decoupling is strong in the case of small solutes, as is observed experimentally. Unfortunately, their theory fails to predict decoupling when the size of the solute is similar to the size of the solvent molecules. In that case, the decoupling could only be explained if solvent heterogeneities are included.

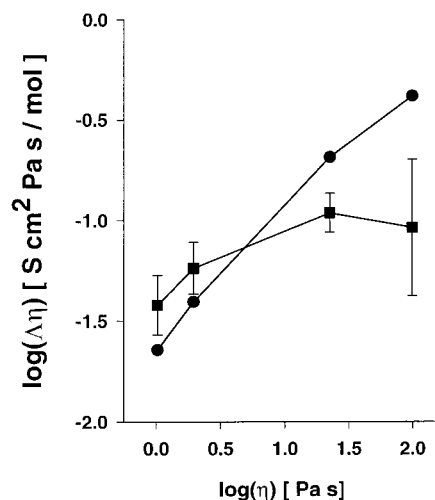


**Figure 4.** Walden plot for concentrated NaCl in aqueous trehalose: (●) experimental and (■) molecular dynamics results.

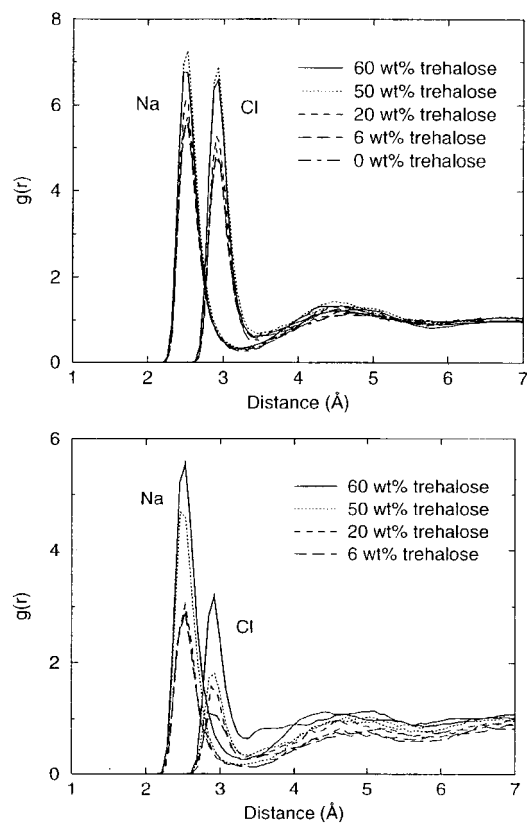


**Figure 5.** Radial distribution functions: (a, top) ion–water and (b, bottom) ion–trehalose OH.

As in our experimental results, molecular dynamics simulations of the diffusion of  $\text{Na}^+$  and  $\text{Cl}^-$  ions in trehalose/water solutions give rise to an increasing  $\Delta\eta$  product with trehalose concentration (Figure 4) and shed some light on the molecular basis of such an effect. Figure 5a shows radial distribution functions of ion/water oxygen as a function of trehalose concentration. Figure 5b shows the corresponding ion/trehalose–hydroxyl distribution functions. At trehalose concentrations above 20 wt %, the height of the first peak of the ion–water pair correlation function increases. That is, the increased concentration of trehalose forces the water closer to the ions. Note, however, that the hydration number of the ions decreases significantly as water is removed from the system. Table 4 gives the hydration number for both trehalose and the ions as a

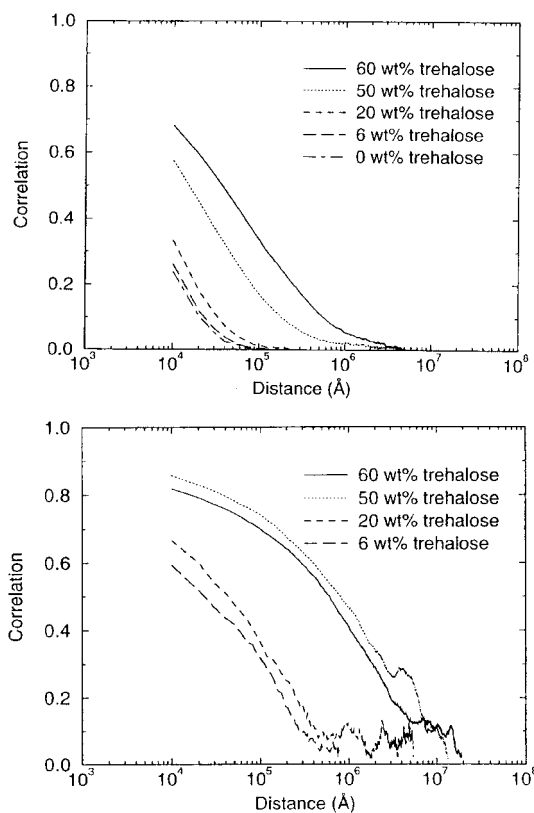


**Figure 6.** Dipole correlation function of water (a, top) and trehalose (b, bottom) as a function of trehalose concentration.

**TABLE 4: Hydration Numbers for Trehalose,  $\text{Na}^+$ , and  $\text{Cl}^-$  at 300 K**

wt % trehalose	trehalose hydration no.	$\text{Na}^+$ hydration no.	$\text{Cl}^-$ hydration no.
0		5.9	6.3
6	15.7	5.2	5.6
20	15.0	5.1	5.6
50	11.9	4.4	5.3
60	11.5	3.4	4.1

function of composition. In the absence of trehalose the hydration number of  $\text{Na}^+$  is about 5.9, while for 60 wt % trehalose solutions it is only 3.4. The height of the first peak of the trehalose–hydroxyl/water distribution function also increases with trehalose concentration (not shown). The structure of these radial distribution functions suggest the formation of small, preferentially solvated regions consisting of an ion, several water molecules, and some of the hydroxyl groups of trehalose. The local environment of the ions therefore contains more water than that corresponding to a uniform distribution (i.e., a disordered, bulk fluid).

Our calculations of the lifetime of ion–water pairs suggest that the residence time of water in the first hydration layer of the ion increases approximately by a factor of 10 as the concentration increases from 6 to 60 wt %. Consequently, the image emerging from molecular dynamic simulations is one of long-lived, local heterogeneities close to the ions, which become more apparent at high trehalose concentrations. These regions are preferentially hydrated and could presumably exhibit a smaller “local viscosity” compared to the bulk value. Figure 6a,b shows the water and trehalose dipole autocorrelation functions as a function of trehalose concentration. These functions can be described by a sum of exponentials; three terms are required for water autocorrelation functions, and two terms are sufficient for trehalose autocorrelation functions. For dilute

trehalose solutions (i.e., 20 wt % trehalose or less), the water dipole autocorrelation function decays to zero in approximately 150 ps. The trehalose dipole autocorrelation function decays to zero in about 1.6 ns, that is, 10 times more slowly than that of water. In more concentrated solutions, (e.g., 60 wt % trehalose) the decay of these functions becomes much slower; for water, the autocorrelation function decays after about 1.6 ns, and for trehalose it decays in more than 12 ns.

The concept of “local viscosity” has been used before to describe dynamic process in liquids.<sup>26,27</sup> Wolynes<sup>26</sup> proposed to write the local viscosity in the form

$$\eta(r) = \eta_0 \left( 1 + \frac{\tau_D(\epsilon_0 - \epsilon_\infty)z^2 e^2}{16\pi\eta_0\epsilon_0 r^4} \right) \quad (6)$$

where  $\epsilon_0$  is the dielectric constant,  $\epsilon_\infty$  is the infinite-frequency dielectric constant,  $\eta_0$  is the bulk viscosity, and  $\tau_D$  is the dipole relaxation time constant. At 300 K, the relaxation time of 60 wt % trehalose is approximately 1 order of magnitude longer than that of water. A simple mixing rule based on the bulk volume fraction composition of the mixture would lead to an overall dipole relaxation time that is dominated by trehalose. In the vicinity of the ions, however, the local composition of water has been shown to be greater than that corresponding to a uniform distribution; the dipole relaxation time would then be dominated by water, resulting in a lower local viscosity. This observation would explain the fact that Walden’s rule is not obeyed for these systems.

There is a growing body of literature that would also support such a hypothesis. In a series of articles<sup>39–41</sup> Lüdemann and co-workers found that the rotational motion (based on spin–lattice relaxation constants,  $T_1$ ) of water in concentrated sucrose becomes highly decoupled from the sucrose or trehalose matrix as the glass transition is approached. This result has recently been extended to self-diffusion constants for trehalose and sucrose in experiments<sup>42</sup> and simulations.<sup>43</sup> These findings would be in agreement with our current observations if the ions are acting as probes for the dynamics of water. In that case, the conductivity of ions in trehalose would be expected to remain higher than Walden behavior would predict owing to the high degree of water mobility even in near-glassy trehalose solutions.

Figure 7a,b shows ion-pair maps for ions in pure water and for ions in concentrated trehalose (60 wt %) solutions. The ordinate axes show the number of ion pairs, defined as any two ions separated by a distance of 3.5 Å or less. The abscissas correspond to the lifetime of individual ion pairs. Whenever an ion pair forms in the system, it is followed in time until it disappears again; in Figure 7, a pairing event is denoted by a horizontal line. A comparison of parts a and b of Figure 7 shows that the frequency of ionic association is comparable in concentrated solutions, but the lifetime of individual pairs is much longer than that in dilute solutions.

## Conclusions

Given the proximity of our measurements to the glass-transition temperature, particularly in the more concentrated trehalose solutions, we are inclined to believe that NaCl is not associated in deeply supercooled liquids. Note, however, that measurements are underway in our laboratory to measure conductivity in amorphous glasses of the systems considered in this work. Simulations have shown the existence of pronounced heterogeneities in aqueous trehalose/NaCl solutions. While the calculations are based on simulations of the liquid state, the experimental observation that the Walden product does

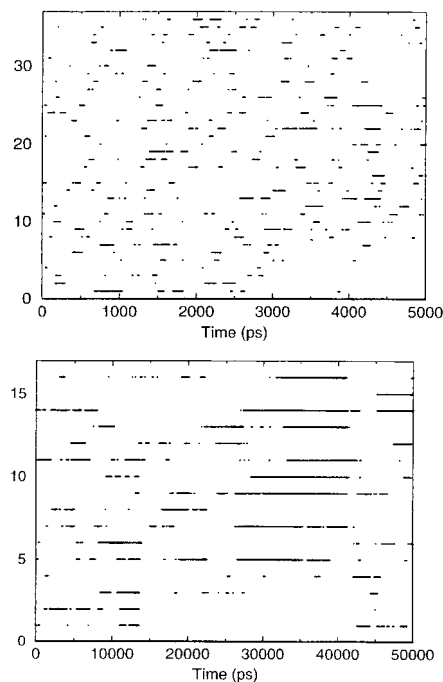


**Figure 7.** Ion-pair maps for (a, top) ions in water and (b, bottom) 60 wt % trehalose aqueous solution. Ordinate value is the pair number (36 possible pairs in (a); 16 possible pairs in (b)).

not change significantly with temperature suggests that such heterogeneities prevail close to  $T_g$ . The picture that emerges from our calculations and experiments is one of slower domains, consisting mostly of trehalose, and faster domains that include the ions and their accompanying hydration shells. Models that attempt to explain the effect of ions on the glass-transition temperature of mixtures of water and cryoprotectants should somehow take into account the nonhomogeneous distribution of water in the vicinity of the ions.

**Acknowledgment.** This work was supported by National Science Foundation Grant CTS9901430.

## References and Notes

- Honadel, T. E.; Killian, G. J. *Cryobiology* **1988**, *25*, 331.
- Crowe, L. M.; et al. *Arch. Biochem. Biophys.* **1985**, *242*, 240.
- Green, J. L.; Angell, C. A. *J. Phys. Chem.* **1989**, *93*, 2880–2882.
- Crowe, L. M.; et al. *Biochim. Biophys. Acta* **1984**, *769*, 141–150.
- Miller, D. P.; de Pablo, J. J. *J. Phys. Chem.*, in press.
- Miller, D. P.; de Pablo, J. J.; Corti, H. R. *J. Phys. Chem. B* **1999**, *103*, 10243.
- Dakhnovskii, Y.; Lubchenko, V. J. *Phys. Chem.* **1996**, *104*, 664–668.
- Shalaev, E. Y.; Franks, F.; Echlin, P. *J. Phys. Chem.* **1996**, *100*, 1144–1152.
- Miller, D. P.; de Pablo, J. J.; Corti, H. R. *J. Chem. Phys.* **1996**, *105* (19), 8979.
- Angell, C. A. *J. Non-Cryst. Solids* **1991**, *131–133*, 13.
- Miller, D. P.; de Pablo, J. J.; Corti, H. *Pharm. Res.* **1997**, *14* (5), 578–590.
- Bird, R. B.; Stewart, W. E.; Lightfoot, E. N. *Transport Phenomena*; John Wiley and Sons: New York, 1960.
- Barthel, J.; et al. *J. Solution Chem.* **1983**, *12*, 449.
- Berendsen, H. J. C.; et al. Interaction models for water in relation to protein hydration. In *Intermolecular Forces*; Pullman, B., Ed.; Reidel: Dordrecht, 1981; pp 331–342.
- Toukan, K.; Rahman, A. *Phys. Rev. B* **1985**, *31* (5), 2645–2648.
- Damm, W.; et al. *J. Comput. Chem.* **1997**, *18* (16), 1955–1970.
- Darden, T.; York, D.; Pedersen, L. *J. Chem. Phys.* **1993**, *98* (12), 10089–10092.
- Essmann, U.; et al. *J. Chem. Phys.* **1995**, *103* (19), 8577–8593.
- Tuckerman, M.; Berne, B. J.; Martyna, G. J. *J. Chem. Phys.* **1992**, *97* (3), 1990–2001.
- Martyna, G. J.; et al. *Mol. Phys.* **1996**, *87* (5), 1117–1157.

- (21) Nosé, S. *J. Chem. Phys.* **1984**, *81* (1), 511–519.
- (22) Robinson, R. A.; Stokes, R. H. In *Electrolyte Solutions*; Butterworth: London, 1959.
- (23) Stokes, R. H. In *The Structure of Electrolytic Solutions*; Hamer, W. J., Ed.; Wiley: New York, 1959; Chapter 20, p 298.
- (24) Moynihan, C. T. *J. Phys. Chem.* **1966**, *70*, 3399–3403.
- (25) Treiner, C.; Fuoss, R. M. *J. Phys. Chem.* **1965**, *69*, 2576–2581.
- (26) Wolynes, P. G. *Annu. Rev. Phys. Chem.* **1980**, *31*, 345–376.
- (27) Bagchi, B.; Biswas, R. *Acc. Chem. Res.* **1998**, *31*, 181–187.
- (28) Pollack, G. L. *Phys. Rev. A* **1981**, *23* (5), 2660–2663.
- (29) Voronel, A.; et al. *Phys. Rev. Lett.* **1998**, *80* (12), 2630–2633.
- (30) McLin, M. G.; Angell, C. A. *J. Phys. Chem.* **1991**, *95*, 9464–9469.
- (31) McLin, M. G.; Angell, C. A. *J. Phys. Chem.* **1996**, *100*, 1181–1188.
- (32) Ehlich, D.; Sillescu, H. *Macromolecules.* **1990**, *23*, 1600–1610.
- (33) Cicerone, M. T.; Ediger, M. D. *J. Chem. Phys.* **1996**, *104* (18), 7210–7218.
- (34) Ediger, M. D. *Annu. Rev. Phys. Chem.*, in press.
- (35) Rössler, E. *Phys. Rev. Lett.* **1990**, *65* (13), 1595–1598.
- (36) Bhattacharyya, S.; Bagchi, B. *J. Chem. Phys.* **1997**, *107* (15), 5852–5862.
- (37) Bhattacharyya, S.; Bagchi, B. *J. Chem. Phys.* **1997**, *106* (5), 1757–1763.
- (38) Sjögren, L.; Sjölander, A. *J. Phys. C: Solid State Phys.* **1979**, *12*, 4369–4392.
- (39) Karger, N.; Ludemann, H.-D. *Z. Naturforsch.* **1991**, *46c*, 313–317.
- (40) Girlich, D.; Ludemann, H.-D. *Z. Naturforsch.* **1993**, *48c*, 407–413.
- (41) Girlich, D.; Ludemann, H.-D. *Z. Naturforsch.* **1994**, *49c*, 250–257.
- (42) Ekdawi, N. C.; Conrad, P. B.; de Pablo, J. J. Submitted for publication in *J. Phys. Chem.*
- (43) Conrad, P. B.; de Pablo, J. J. *J. Phys. Chem.* **1999**, *103*, 4049–4055.
- (44) Nicolajsen, H.; Hvidt, A. *Cryobiology* **1994**, *31*, 199.
- (45) Saleki-Gerhardt, A. Ph.D. Thesis, Pharmacy Department, University of Wisconsin, Madison, WI, 1993.